

Identifying Radiological Findings Related to COVID-19 from Medical Literature

Yuxiao Liang
UC San Diego

YUL154@ENG.UCSD.EDU

Pengtao Xie
UC San Diego

PENGTAOXIE2008@GMAIL.COM

Abstract

Coronavirus disease 2019 (COVID-19) has infected more than one million individuals all over the world and caused more than 55,000 deaths, as of April 3 in 2020. Radiological findings are important sources of information in guiding the diagnosis and treatment of COVID-19. However, the existing studies on how radiological findings are correlated with COVID-19 are conducted separately by different hospitals, which may be inconsistent or even conflicting due to population bias. To address this problem, we develop natural language processing methods to analyze a large collection of COVID-19 literature containing study reports from hospitals all over the world, reconcile these results, and draw unbiased and universally-sensible conclusions about the correlation between radiological findings and COVID-19. We apply our method to the COVID-19 dataset and successfully extract a set of radiological findings that are closely tied to COVID-19.

1. Introduction

Coronavirus disease 2019 (COVID-19) is an infectious disease that has affected more than one million individuals all over the world and caused more than 55,000 deaths, as of April 3 in 2020. The science community has been working very actively to understand this new disease and make diagnosis and treatment guidelines based on the findings. One major stream of efforts are focused on discovering the correlation between radiological findings in the lung areas and COVID-19. There have been several works (Liu et al.; Li and Xia) publishing such results. However, existing studies are mostly conducted separately by different hospitals and medical institutes. Due to geographic affinity, the populations served by different hospitals have different genetic, social, and ethnic characteristics. As a result, the radiological findings from COVID-19 patient cases in different populations are different. This population bias incurs inconsistent or even conflicting conclusions regarding the correlation between radiological findings and COVID-19. As a result, medical professionals cannot make informed decisions on how to use radiological findings to guide diagnosis and treatment of COVID-19.

We aim to address this issue. Our research goal is to develop natural language processing methods to collectively analyze the study results reported by many hospitals and medical institutes all over the world, reconcile these results, and make a holistic and un-

biased conclusion regarding the correlation between radiological findings and COVID-19. Specifically, we take the CORD-19 dataset (Inc., 2020), which contains over 45,000 scholarly articles, including over 33,000 with full text, about COVID-19, SARS-CoV-2, and related coronaviruses. We develop sentence classification methods to identify all sentences narrating radiological findings from COVID-19. Then constituent parsing is utilized to identify all noun phrases from these sentences and these noun phrases contain abnormalities, lesions, diseases identified by radiology imaging such as X-ray and computed tomography (CT). We calculate the frequency of these noun phrases and select those with top frequencies for medical professionals to further investigate. Since these clinical entities are aggregated from a number of hospitals all over the world, the population bias is largely mitigated and the conclusions are more objective and universally informative. From the CORD-19 dataset, our method successfully discovers a set of clinical findings that are closely related with COVID-19.

The major contributions of this paper include:

- We develop natural language processing methods to perform unbiased study of the correlation between radiological findings and COVID-19.
- We develop a bootstrapping approach to effectively train a sentence classifier with light-weight manual annotation effort. The sentence classifier is used to extract radiological findings from a vast amount of literature.
- We conduct experiments to verify the effectiveness of our method. From the CORD-19 dataset, our method successfully discovers a set of clinical findings that are closely related with COVID-19.

The rest of the paper is organized as follows. In Section 2, we introduce the data. Section 3 presents the method. Section 4 gives experimental results. Section 5 concludes the paper.

2. Dataset

We used the COVID-19 Open Research Dataset (CORD-19) (Inc., 2020) for our study. In response to the COVID-19 pandemic, the White House and a coalition of research groups prepared the CORD-19 dataset. It contains over 45,000 scholarly articles, including over 33,000 with full text, about COVID-19, SARS-CoV-2, and related coronaviruses. These articles are contributed by hospitals and medical institutes all over the world. Since the outbreak of COVID-19 is after November 2019, we select articles published after November 2019 to study, which include a total of 2081 articles and about 360000 sentences. Many articles report the radiological findings related to COVID-19. Table 1 shows some examples.

3. Methods

Our goal is to develop natural language processing (NLP) methods to analyze a large collection of COVID-19 literature and discover unbiased and universally informative correlation between radiological findings and COVID-19. To achieve this goal, we need to address two technical challenges. First, in the large collection of COVID-19 literature, only a small

Table 1: Example sentences describing radiological findings related with COVID-19

The X-ray chest and Highresolution computed-tomography chest showed a progressively reduced bilateral pleural effusion, interstitial-alveolar edema with bilateral hilar congestion.
Non-pleural effusion appeared in the first and second CT examination and a bilateral pleural effusion appeared in the third CT examination.
Chest CT scans revealed that the grade 2 lesion and one of the grade 3 lesions as areas of prominent breast tissue mimicking faint GGO and post-inflammatory focal atelectasis on chest radiography, respectively.
A showed many CT features such as ground-glass opacification, cobblestone/reticular pattern (blue arrow and blue line around region), fibrosis and dilated bronchi with thickened wall (the enlarged image in the upper right corner, red arrow).
The typical CT images show bilateral pulmonary parenchymal ground-glass and consolidative pulmonary opacities, sometimes with a rounded morphology and a peripheral lung distribution.
The chest CT (Figure 3) showed multi-focal GGO with parenchyma consolidation and subpleural effusion, predominantly involving upper lungs.

part of sentences are about radiological findings. It is time-consuming to manually identify these sentences. Simple methods such as keyword-based retrieval will falsely retrieve sentences that are not about radiological findings and miss sentences that are about radiological findings. How can we develop NLP methods to precisely and comprehensively extract sentences containing radiological findings with minimum human annotation? Second, given the extracted sentences, they are still highly unstructured, which are difficult for medical professionals to digest and index. How can we further process these sentences into structured information that is more concise and easy to use?

To address the first challenge, we develop a sentence classifier to judge whether a sentence contains radiological findings. To minimize manual-labeling overhead, we propose easy ways of constructing positive and negative training examples, develop a bootstrapping approach to mine hard examples, and use hard examples to re-train the classifier for reducing false positives. To address the second challenge, we use constituent parsing to recognize noun phrases which contain critical medical information (e.g., lesions, abnormalities, diseases) and are easy to index and digest. We select noun phrases with top frequencies for medical professionals to further investigate.

3.1. Extracting Sentences Containing Radiological Findings

In this section, we develop a sentence-level classifier to determine whether a sentence contains radiological findings. To build such a classifier, we need to create positive and negative training sentences, without labor-intensive annotations. To obtain positive examples, we resort to the MedPix¹ database, which contains radiology reports narrating radiological findings. MedPix is an open-access online database of medical images, teaching cases, and clinical topics. It contains more than 9000 topics, 59000 images from 12000 patient cases. We selected diagnostic reports for CT images and used sentences in the reports as positive samples. To obtain negative sentences, we randomly sample some sentences from the arti-

1. <https://medpix.nlm.nih.gov/home>

cles and quickly screen them to ensure that they are not about radiological findings. Since most sentences in the literature are not about radiological findings, a random sampling can almost ensure the select sentences are negative. A manual screening is conducted to further ensure this and the screening effort is not heavy.

Given these positive and negative training sentences, we use them to train a sentence classifier which predicts whether a sentence is about the radiological findings of COVID-19. We use the Bidirectional Encoder Representations from Transformers (BERT) (Devlin et al., 2018) model for sentence classification. BERT is a neural language model that learns contextual representations of words and sentences. BERT pretrains deep bidirectional representations from unlabeled text by jointly conditioning on both left and right context in all layers. To apply the pretrained BERT to a downstream task such as sentence classification, one can add an additional layer on top of the BERT architecture and train this newly-added layer using the labeled data in the target task. In our case, similar to (Lee et al., 2020), we pretrain the BERT model on a vast amount of biomedical literature to obtain semantic representations of words. A linear layer is added to the output of BERT for predicting whether this sentence is positive (containing radiological finding) or negative. The architecture and hyperparameters of the BERT model used in our method are the same as those in (Lee et al., 2020). Figure 1 shows the architecture of the classification model.

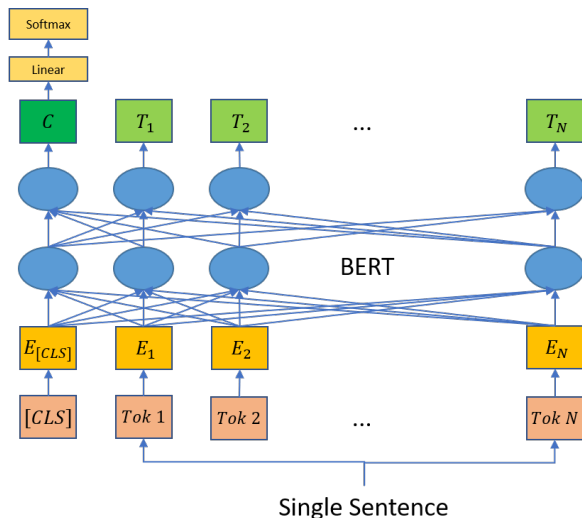


Figure 1: Architecture of the sentence classification model.

When applying this trained sentence classifier to unseen sentences, we found that it yields a lot of false positives: many sentences irrelevant to radiological findings of COVID-19 are predicted as being relevant. To solve this problem, we iteratively perform hard example mining in a bootstrapping way and use these hard examples to retrain the classifier for reducing false positives. At iteration t , given the classifier C_t , we apply it to make predictions on unseen sentences. Each sentence is associated with a prediction score where a larger score indicates that this sentence is more likely to be positive. We rank these sentences in descending order of their prediction scores. Then for the top-K sentences with the largest prediction scores, we read them and label each of them as either being positive

or negative. Then we add the labeled pairs to the training set and re-train the classifier and get C_{t+1} . This procedure is repeated again to identify new false positives and update the classifier using the new false positives.

3.2. Extracting Noun Phrases

The extracted sentences containing radiological findings of COVID-19 are highly unstructured, which are still difficult to digest for medical professionals. To solve this problem, from these unstructured sentences, we extract structured information that is both clinically important and easy to use. We notice that important information, such as lesions, abnormalities, diseases, is mostly contained in noun phrases. Therefore, we use NLP to extract noun phrases and perform further analysis therefrom. First, we perform part-of-speech (POS) tagging to label each word in a sentence as being a noun, verb, adjective, etc. Then on top of these words and their POS tags, we perform constituent parsing to obtain the syntax tree of the sentence. An example is shown in Figure 2. From bottom to top of the tree, fine-grained linguistic units such as words are composed into coarse-grained units such as phrases, including noun phrases. We obtain the noun phrases by reading the node labels in the tree.

Given the extracted noun phrases, we remove stop words in them and perform lemmatization to eliminate non-essential linguistic variations. We count the frequency of each noun phrase and rank them in descending frequency. Then we select the noun phrases with top frequencies and present them to medical professionals for further investigation.

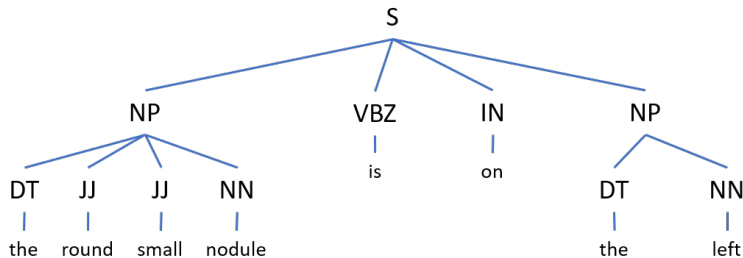


Figure 2: An example of constituent parse tree.

4. Experiment

4.1. Experimental Settings

For building the initial sentence classifier (before hard-example mining), we collected 2350 positive samples from MedPix and 3000 negative samples from CORD-19. We used 90% sentences for training and the rest 10% sentences for validation. The weights in the sentence classifier are optimized using the Adam algorithm with a learning rate of 2×10^{-5} and a mini-batch size of 4. In bootstrapping for hard example mining, we added 400 false positives in each iteration for classifier-retraining and we performed 4 iterations of bootstrapping.

4.2. Results of Sentence Classification

Under the final classifier, 998 sentences are predicted as being positive. Among them, 717 are true positives (according to manual check). The classifier achieves a precision of 71.8%. For the initial classifier (before adding mined hard examples using bootstrapping), among the top 100 sentences with the largest prediction scores, 53 are false positives. The initial classifier only achieves a precision of 47%. The precision achieved by classifiers trained after round 1-3 in bootstrapping is 55%, 57%, and 69% respectively, as shown in Table 2. This demonstrates the effectiveness of hard example mining. Table 3 shows some example sentences that are true positives, true negatives, and false positives, under the predictions made by the final classifier.

Table 2: Precision at top-100 after each iteration

Iteration	Precision
0	47%
1	55%
2	57%
3	69%

4.3. Results of Noun Phrase Extraction

Table 4 shows the extracted noun phrases with top frequencies that are relevant to radiology. Medical professionals can look at this table and select noun phrases indicating radiological findings for further investigation, such as consolidation, pleural effusion, ground glass opacity, thickening, etc. We mark such noun phrases with bold font in the table. To further investigate how a noun phrase is relevant to COVID-19, medical professionals can review the sentences mentioning this noun phrase. Table 5,6,7 show some examples.

For example, reading the five example sentences containing consolidation, one can judge that consolidation is a typical manifestation of COVID-19. This is in accordance with the conclusion in (Kanne et al., 2020): “Consolidation becomes the dominant CT findings as the disease progresses.” Similarly, the example sentences of pleural effusion, ground glass opacity, thickening, fibrosis, bronchiectasis, lymphadenopathy show that these abnormalities are closely related with COVID-19. This is consistent with the results reported in the literature:

- **Pleural effusion:** “In terms of pleural changes, CT showed that six (9.7%) had pleural effusion.” (Zhou et al., 2020)
- **Ground glass opacity:** “The predominant pattern of abnormalities after symptom onset was ground-glass opacity (35/78 [45%] to 49/79 [62%] in different periods.” Wang et al. (2020)
- **Thickening:** “Furthermore, ground-glass opacity was subcategorized into: (1) pure ground-glass opacity; (2) ground-glass opacity with smooth interlobular septal thickening.” (Wang et al., 2020)

Table 3: Example sentences for true positive (TP), true negative (TN), and false positive (FP).

TP	Her chest radiograph demonstrated no abnormalities, but a CT scan of her chest revealed bilateral multifocal infiltrates and mediastinal and hilar lymphadenopathy.
	The predominant pattern was groundglass opacity, with illdefined margins, air bronchograms, smooth or irregular inter lobular or septal thickening, and thickening of the adjacent pleura.
	The patient’s chest CT showed pulmonary consolidation, interlobular septal thickening, and pleural effusion.
	Dynamic imaging showed progressive multi-spot patchy shadows in both lungs.
TN	Fourth, leisure activities and training on how to relax were properly arranged to help staff reduce stress.
	Uncertainties of discrete E. coli samples and flow measurements were N30 and 97%, respectively.
	Acute lower respiratory tract infections (ALRIs) are a common illness in children < 5 years old, with significant morbidity and mortality in infants and young children under the age of two (1) (2) (3)
	Bovine viral diarrhea (BVD), which is caused by BVD virus (BVDV) infection, is one of the most important viral diseases of cattle, causing enormous economic losses to the livestock industry worldwide (Suda et al., 2018) .
FP	Pathology: At necropsy, there is diffuse lymphoma affecting multiple organs that can include those noted above plus kidney, adrenal gland, tonsils, and lung.
	The stoma site per se is an incisional hernia by definition as it is a defect in the abdominal fascia with protruding intra-abdominal contents.
	He was diagnosed with coronary artery disease in last year and was stented in Left anterior descending artery.
	Ultimately, the patient underwent mitral valve replacement following the stress test.

Table 4: Extracted radiology-relevant noun phrases with top phrases. Noun phrases relevant to clinical findings are highlighted with bold font.

Noun phrase	Frequency	Noun phrase	Frequency
ct	103	liver	19
consolidation	79	fibrosis	13
lung	62	abscess	13
lobe	61	infection	13
chest	57	air bronchogram	12
pleural effusion	54	lymphadenopathy	12
ground glass opacity	53	hrct	11
lesion	50	interlobular septa	11
chest x-ray	38	cxr	10
pneumonia	35	trachea	10
chest radiographs	29	bronchiectasis	9
tomography	27	fever	5
echocardiogram	22	multiple sclerosis	3
thickening	21		

- **Fibrosis:** “In five patients, follow-up CT showed improvement with the appearance of fibrosis and resolution of GGOs.”, (Li and Xia, 2020)
- **Bronchiectasis and lymphadenopathy:** “The most common patterns seen on chest CT were ground-glass opacity, in addition to ill-defined margins, smooth or irregular interlobular septal thickening, air bronchogram , crazy-paving pattern, and thickening of the adjacent pleura. Less common CT findings were nodules, cystic changes, bronchiolectasis, pleural effusion , and lymphadenopathy.” (Shi et al., 2020)

5. Conclusions

In this paper, we develop natural language processing methods to automatically extract unbiased radiological findings of COVID-19. We develop a BERT-based classifier to select sentences that contain COVID-related radiological findings and use bootstrapping to mine hard examples for reducing false positives. Constituent parsing is used to extract noun phrases from the positive sentences and those with top frequencies are selected for medical professionals to further investigate. From the CORON-19 dataset, our method successfully discovers radiological findings that are closely related with COVID-19.

References

Jacob Devlin, Ming-Wei Chang, Kenton Lee, and Kristina Toutanova. Bert: Pre-training of deep bidirectional transformers for language understanding. *arXiv preprint arXiv:1810.04805*, 2018.

Table 5: Example sentences containing interested noun phrases

consolidation	Chest CT images showed diffuse irregular small diffuse ground-glass nodular opacities with partial consolidation in bilateral lungs on Day 10 (Figure 1A).
	Axial thin-section non-contrast CT scan shows diffuse bilateral confluent and patchy ground-glass, air-bronchogram and consolidation , characterized by peripheral distribution.
	B showed consolidation (pink arrow) and mixed pattern (yellow arrow and yellow line around region) in the bilateral lower lobes.
	Subsequent chest CT images showed bilateral groundglass opacity, whereas the consolidation was resolved.
	CT scan revealed bilateral peribronchial consolidation , swollen jejunum lymph node with uniform distribution of contrast medium, and multiple prominent nodules of the liver.
pleural effusion	The chest film is not helpful in making a specific etiologic diagnosis; however, lobar consolidation, cavitation, and large pleural effusions support a bacterial cause.
	Inhalation anthrax is notable for its absence of pulmonary infiltrate on chest imaging, but the presence of extensive mediastinal lymphadenopathy, pleural effusions , and severe shortness of breath, toxemia, and sense of impending doom.
	An echocardiogram showed severe reduction of the left ventricular (LV) ejection fraction (25%) and a chest X-ray exhibited bilateral pleural effusion with pulmonary interstitial edema (Fig).
	The patient received 2 g/kg IVIG and significant pleural effusion was noted on the chest radiography and computed tomography 48 h after the completion of therapy.
	Chest computed tomography showed bilateral pleural effusion , bilateral consolidation with air bronchogram, and ground-glass opacities in her left lung (Fig).
ground-glass opacity	Axial thin-section non-contrast CT image shows diffusion lesions in bilateral lung, mainly manifested as ground-glass opacification (red arrow and red line around region),and cobblestone/Reticular pattern(blue arrow and blue line around region).
	Chest CT will show areas of ground-glass opacity and consolidation in involved segments.
	CT findings included ground glass opacity, consolidation, air bronchogram and nodular opacities.
	CT images were reviewed and scored for lesion distribution, lobe and segment involvement, ground-glass opacities , consolidation, and interstitial thickening.
	The most frequent radiological patterns on plain chest radiography was airspace/ ground glass opacification in various lobes.
thickening	Most of the lesions were distributed along the bronchovascular bundle or the dorso-lateral and subpleural part of the lungs and were seen with or without interlobular septal thickening .
	CT images were reviewed and scored for lesion distribution, lobe and segment involvement, ground-glass opacities, consolidation, and interstitial thickening .
	Chest radiographs often demonstrate peribronchial thickening and infiltrates, often with areas of atelectasis.
	Other c-HRCT signs of bronchiectasis include abnormalities in the surrounding lung may include parenchyma loss, emphysema, scars and nodular foci, 150 a linear array or cluster of cysts, dilated bronchi in the periphery of the lung, and bronchial wall thickening (Box 26.1).
	CT showed multiple peripheral lesions in bilateral lungs, mainly characterized by GGO, paving stones and vascular thickening .

Table 6: Example sentences containing interested noun phrases

fibrosis	(D) Images obtained 5 days later showed partial absorption of the consolidation lesions in the right lower lobe, but fibrosis , bronchiectasis, and vascular thickening occurred.
	High-resolution chest computer tomography (HRCT) presented diffuse ground glass opacities, intra-lobular reticulation and small cysts in the upper lobes, middle lobe and lingula, suggesting pulmonary fibrosis (Fig.
	These findings indicated the appearance of interstitial changes, suggesting the development of fibrosis .
	No other clinical or radiological changes of lung congestion, fibrosis , or cancer to explain these ground-glass lung changes, or any concomitant radiological changes of dense consolidation, pleural effusion, lymphadenopathy, or pneumomediastinum were seen.
	If the diagnosis of idiopathic pulmonary fibrosis is not previously established this criterion can be met by the presence of radiologic and/or histopathologic changes consistent with usual interstitial pneumonia pattern on the current evaluation.
abscess	A contrast-enhanced computed tomography scan is useful because it differentiates a fully developed abscess from cellulitis and delineates the full extent of the abscess.
	The abscess pushes the adjacent tonsil downward and medially, and the uvula may be so edematous, as to resemble a white grape.
	A CT of the neck was obtained to rule out other etiologies for respiratory distress, which was negative for peritonsillar or retropharyngeal abscess .
	Abnormalities include bronchopneumonia, solitary or multiple lung nodes, miliary interstitial lung disease, lung abscess , and pleural effusion.
	A lung abscess, like an abscess elsewhere, represents a localized collection of pus.
air bronchogram	CT findings included ground glass opacity, consolidation, air bronchogram and nodular opacities.
	Chest CT on Jan 13 showed improved status (3B) with diffuse consolidation of both lungs, uneven density and air bronchogram .
	Chest computed tomography showed bilateral pleural effusion, bilateral consolidation with air bronchogram , and ground-glass opacities in her left lung (Fig.
	The predominant pattern was groundglass opacity, with illdefined margins, air bronchograms , smooth or irregular inter lobular or septal thickening, and thickening of the adjacent pleura.
	Computed tomography axial (A) and coronal (B) plane revealed multiple lesions (arrows) of ground glass opacity accompanied with consolidation under or near the pleura in bilateral lower lobes, with air bronchogram and thickened interlobular septa.
lymphadenopathy	Merely consolidation, central distribution only, pleural effusions or lymphadenopathy were relatively rarely seen.
	Thoracic and abdominal radiographs may provide evidence of pulmonary lesions, lymphadenopathy , and/or hepatosplenomegaly.
	Neither pleural effusion nor lymphadenopathy was found.
	Neither patient showed pleural effusion or lymphadenopathy .
	3.1 presence of lymphadenopathy (defined as lymph node size of !10 mm in short-axis dimension); 3.2 presence of pericardial effusion; 3.3 ascending thoracic aorta diameter.

Table 7: Example sentences containing interested noun phrases

intralobular septa	The lesion density was mostly non-uniform with air bronchogram and thickened interlobular or intralobular septa .
	The lesion may be patchy, nodular, honeycomb, grid or strips, and the lesion density is mostly uneven with the primary presentation of ground glass opacity accompanied by thickening of interlobular or intralobular septa .
	High-resolution CT might show ground glass opacities (figure 5B) in early CT findings (with or without consolidation) followed by interlobular septal and intralobular interstitial thickening with peripheral and lower lobe involvement 93, 94 within the first week of MERS-CoV infection.
	Other findings included intralobular or interlobular septal thickening, and a crazy paving pattern.
	Most of the lesions were distributed along the bronchovascular bundle or the dorsolateral and subpleural part of the lungs and were seen with or without interlobular septal thickening.
trachea	A lateral neck radiograph may show a hazy tracheal air column, with multiple luminal soft tissue irregularities due to pseudomembrane detachment from the soft tissue, but radiographs should be taken only after the patient is stabilized and safe.
	CT imaging demonstrated diffuse edema and narrowing of the glottis, subglottis, and upper trachea in keeping with croup.
	Tracheal intubation was seen in the trachea and the heart shadow outline was not clear.
	Black arrows in the trachea indicate cilia and necrosis loss.
	A neck radiograph will show the traditional narrowing of the trachea known as a steeple sign.
bronchiectasis	The timing of c-HRCT scans to diagnose bronchiectasis is important.
	Other c-HRCT signs of bronchiectasis include abnormalities in the surrounding lung may include parenchyma loss, emphysema, scars and nodular foci, 150 a linear array or cluster of cysts, dilated bronchi in the periphery of the lung, and bronchial wall thickening (Box 26.1).
	In particular, CT is much better at identifying the presence and extent of bronchiectasis compared with thoracic radiography.
	(D) Images obtained 5 days later showed partial absorption of the consolidation lesions in the right lower lobe, but fibrosis, bronchiectasis , and vascular thickening occurred.
	In the right upper lobe, there were ground glass densification areas, traction bronchiectasis , interlobular septa thickening and subpleural cystic lesions.

- Scite Inc. Cord-19_ scite_citation_tallies+contexts, March 2020. URL <https://doi.org/10.5281/zenodo.3724818>.
- Jeffrey P Kanne, Brent P Little, Jonathan H Chung, Brett M Elicker, and Loren H Ketai. Essentials for radiologists on covid-19: an updaterradiology scientific expert panel, 2020.
- Jinhyuk Lee, Wonjin Yoon, Sungdong Kim, Donghyeon Kim, Sunkyu Kim, Chan Ho So, and Jaewoo Kang. Biobert: a pre-trained biomedical language representation model for biomedical text mining. *Bioinformatics*, 36(4):1234–1240, 2020.
- Yan Li and Liming Xia. Coronavirus disease 2019 (covid-19): Role of chest ct in diagnosis and management. *American Journal of Roentgenology*, pages 1–7.
- Yan Li and Liming Xia. Coronavirus disease 2019 (covid-19): Role of chest ct in diagnosis and management. *American Journal of Roentgenology*, pages 1–7, 2020.
- Huanhuan Liu, Fang Liu, Jinning Li, Tingting Zhang, Dengbin Wang, and Weishun Lan. Clinical and ct imaging features of the covid-19 pneumonia: Focus on pregnant women and children. *Journal of Infection*.
- Heshui Shi, Xiaoyu Han, Nanchuan Jiang, Yukun Cao, Osamah Alwalid, Jin Gu, Yanqing Fan, and Chuansheng Zheng. Radiological findings from 81 patients with covid-19 pneumonia in wuhan, china: a descriptive study. *The Lancet Infectious Diseases*, 2020.
- Yuhui Wang, Chengjun Dong, Yue Hu, Chungao Li, Qianqian Ren, Xin Zhang, Heshui Shi, and Min Zhou. Temporal changes of ct findings in 90 patients with covid-19 pneumonia: A longitudinal study. *Radiology*, page 200843, 2020.
- Shuchang Zhou, Yujin Wang, Tingting Zhu, and Liming Xia. Ct features of coronavirus disease 2019 (covid-19) pneumonia in 62 patients in wuhan, china. *American Journal of Roentgenology*, pages 1–8, 2020.